Reversible Morphological Transitions of Polystyrene-*b*-polyisoprene Micelles

Isaac LaRue,† Mireille Adam,† Marinos Pitsikalis,‡ Nikos Hadjichristidis,‡ Michael Rubinstein,† and Sergei S. Sheiko*,†

Department of Chemistry, University of North Carolina at Chapel Hill, Chapel Hill, North Carolina 27599-3290, and Department of Chemistry, University of Athens, Panepistimiopolis, Zografou, 157 71 Athens, Greece

Received July 15, 2005; Revised Manuscript Received October 22, 2005

ABSTRACT: Reversible morphological transitions of diblock copolymer micelles in dilute solutions were monitored by light scattering and atomic force microscopy for two different polymer samples near the calculated morphological boundaries. These transitions were induced solely by temperature changes. At 25 °C, a sample of polystyrene-*b*-polyisoprene diblock micelles with a polystyrene block of 20.6 kDa and a polyisoprene block of 6 kDa was observed to form cylindrical micelles in heptane, a selective solvent for polyisoprene. Upon heating to 35 °C, the sample adopted a spherical micelle morphology. When the sample was cooled back to 25 °C, cylindrical micelles were once again observed. In addition, a reversible transition from vesicles to cylindrical micelles, upon heating from 25 to 40 °C, was observed for a second diblock sample with the same polystyrene block (20.6 kDa) and a shorter polyisoprene block of 4.3 kDa. The change in morphology upon heating was found to be much faster then the reverse process upon cooling.

Introduction

When diblock polymers are dissolved in a selective solvent (good solvent for one block and poor solvent for the other) above a certain concentration, called the critical micelle concentration (cmc), the diblocks will associate to form micelles with a core of the insoluble blocks and a corona of the soluble blocks.[1−5] If the diblocks have a large soluble block, spherical micelles are typically formed. As the molecular weight of the soluble block is decreased (while the molecular weight of the insoluble block remains constant), theory predicts a transition between spherical micelles and wormlike cylindrical micelles and eventually to vesicles. Recently developed theory can be used to calculate the location of the boundaries between the different micelle morphologies.[6]

Figure 1 shows the phase diagram wherein the boundaries between the cylindrical and lamella morphologies and spherical and cylindrical morphologies are given by

$$N_A^{cl} = \left(\frac{\pi^2 N_B^{\,2}}{2p_B\varphi^3}\right)^{1/3} \frac{\gamma^{1/3}}{C_H {p_A}^{1/3}\nu^{1/3}} \left(\frac{a_B}{a_A}\right)^{5/3} \left(\frac{5C_F}{6}\right)^{-2/3} \quad (1)$$

$$N_A^{sc} = C_U N_A^{cl} \quad (2)$$

where N_A, a_A, p_A and N_B, a_B, p_B are respectively the degree of polymerization, the monomer size, and the stiffness parameter of the soluble and insoluble blocks.[6] The stiffness parameter is defined as $p = l/a$, where l is the length of the Kuhn segment and a is the monomer size. In this paper, we used the handbook data $a_A = 5$ Å, $p_A = 1.6$ and $a_B = 5.6$ Å, $p_B = 1.5$ for PI and PS blocks, respectively. The other parameters, such as ν, the excluded volume parameter of the soluble block, γ, the surface free energy per area $a_B{}^2$ of the insoluble core, and φ, the volume fraction of insoluble monomer in the micelle core, were experimentally measured.[6] Equation 1 includes two numerical coefficients $C_F = 1.38$ and $C_H = 1.13$ on the order of unity defined in ref 6. The C_F value was determined in ref 6, whereas C_H was adjusted to the experimental data obtained in this work. In eq 2, we introduced additional coefficient C_U which signifies the theoretical prediction[6] of the universal width of the stability range of cylindrical micelles defined as $\Delta N_A/N_A^{cl}$. In this paper, we used $C_U = 1 + \Delta N_A/N_A^{cl} = 1.37$, which was experimentally measured for two different sets of PS-*b*-PI diblocks and found between the asymptotic value $C_U = 1.31$ and numerical solution

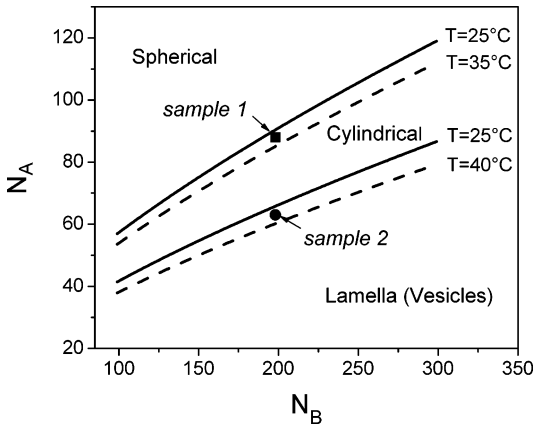

Figure 1. Phase diagram for PS-*b*-PI in heptane shows the temperature variation in the spherical−cylindrical (S−C) and cylindrical−lamella (C−L) morphological boundaries calculated from using eq 2 and eq 1, respectively. The solid lines are calculated for $T = 25$ °C, and the dashed lines are calculated for $T = 35$ °C (S−C boundary) and for $T = 40$ °C (C−L boundary). The model parameters used are $a_B = 5.6$ Å, $a_A = 5.0$ Å, $p_B = 1.5$, $p_A = 1.6$, $\varphi = 0.7$, $C_F = 1.38$, $C_H = 1.13$, and $C_U = 1.37$ with γ and ν being determined for each temperature using eqs 3 and 4. When changing temperature, the phase boundaries shift across sample 1 (solid circle) and sample 2 (solid square) from solid lines to dashed lines inducing morphological transitions in these samples.

† University of North Carolina at Chapel Hill.
‡ University of Athens.
* To whom correspondence should be addressed. E-mail: sergei@email.unc.edu.

10.1021/ma051548z CCC: $33.50
Published on Web 11/19/2005

Table 1. Molecular Characteristics of the Samples

sample	$(M_w)_{PS\ block}{}^a \times 10^{-3}$	$(M_w)_{PI\ block}{}^b \times 10^{-3}$	$(M_w)_{diblock}{}^a \times 10^{-3}$	$M_w/M_n{}^c$	dn/d$c{}^d$ (mL g^{-1})	wt % PS^e
1	20.6	4.3	24.9	1.03	0.177	83.0
2	20.6	6.0	26.6	1.04	0.174	77.1

[a] By LALLS. [b] Calculated as $(M_w)_{diblock} - (M_w)_{PS\ block}$. [c] By GPC. [d] By differential refractometry. [e] By ^{1}H NMR.

$C_U = 1.50$ obtained by minimization of the full expression for the micelle free energy.[6]

As follows from eqs 1 and 2, changes in any of the various parameters can cause the morphological boundaries to shift. The change in micelle morphology by reducing the size of the soluble block, while keeping the insoluble block size constant, has been experimentally verified.[6−11] In addition to changing the ratio of the blocks, it has been previously shown that morphological transitions take place with the addition of a corelike homopolymer[12] and changing the solvent quality for the core and/or corona blocks through the addition of cosolvent.[13−16] While these studies show that it is possible to change from one morphology to another, the only way to recover the original morphology is through the addition of more solvent or diblock. Here we show that similar morphological transitions are induced by changing temperature while keeping the solvent and polymer concentration constant. Atomic force microscopy and light scattering data demonstrate that reversible transformations from cylindrical to spherical micelles and from vesicle to cylindrical micelles take place upon the heating and subsequent cooling of dilute solutions of polystyrene-*b*-polyisoprene copolymer in heptane. The observed transitions are attributed to the temperature dependence of the excluded volume parameter ν of the soluble PI block and the surface free energy γ of the insoluble PS block. In principle, this is similar to changing ν and γ through the addition of cosolvent, but it has the advantage that only temperature, i.e., an intensive parameter, is being changed without affecting the solution composition.

Experimental Section

Materials. We studied two diblock copolymers, PS-*b*-PI, of polystyrene (PS) and polyisoprene (PI) with the same PS block (21.6 kDa) and different PI blocks (6 and 4.3 kDa). Molecular characteristics of the copolymers are given in Table 1. The microstructure of the PI block for both samples was 93% of 1,4-poly(isoprene) and 7% of 3,4-poly(isoprene).

The diblock copolymers were synthesized by sequential anionic polymerization high-vacuum techniques.[17] Styrene was polymerized first in benzene at room temperature using *sec*-BuLi as initiator. A small quantity of the living polystyrene, PSLi, solution was sampled for characterization, and the rest was divided to calibrated cylinders, which were removed from the polymerization apparatus by heat sealing. The PSLi content of each cylinder was used to initiate the polymerization of a predetermined amount of isoprene in separate polymerization apparatuses in order to prepare PS-*b*-PI block copolymers with the desired molecular weight of the PI block. The copolymers were precipitated in methanol and fractionated in toluene/methanol as the solvent/nonsolvent system in order to remove traces of deactivated PS block during the synthesis. The purified copolymers were precipitated in methanol and dried under vacuum.

Characterization. The samples were characterized by size exclusion chromatography (SEC) and low angle laser light scattering (LALLS). SEC experiments were conducted at 40 °C using a modular instrument consisting of a Waters model 510 pump, a Waters model U6K sample injector, a Waters model 401 differential refractometer, a Waters model 486 UV spectrophotometer, and a set of 4 μm Styragel columns with a continuous porosity range from 10^6 to 10^3 Å. The columns were housed in an oven thermostated at 40 °C. THF was the carrier solvent at a flow rate of 1 mL/min.

The LALLS measurements were performed with a Chromatix KMX-6 low angle laser light scattering photometer at 25 °C equipped with a 2 mW He−Ne laser operating at $\lambda = 633$ nm. The equation describing the concentration dependence of the reduced intensity is

$$Kc/\Delta R_\theta = 1/M_{w,app} + 2A_2c + ...$$

where ΔR_θ is the excess Rayleigh ratio of the solution over that of the solvent and K is a combination of optical and physical constants, including the refractive index increment dn/dc. Stock solutions were prepared, followed by dilution with solvent to obtain appropriate concentrations. All solutions and solvents were purified by filtering through 0.22 μm pore size nylon filters directly into the scattering cell. Refractive index increments, dn/dc, at 25 °C were measured with a Chromatix KMX-16 refractometer operating at 633 nm and calibrated with aqueous NaCl solutions.

The purity of the sample (i.e., lack of homopolymers) was verified by dynamic light scattering, the procedure of which is detailed in the Supporting Information of a previous publication.[11] All solvents used for the micelle characterization were purchased from Fisher Chemicals or Acros Organics and were filtered through 0.2 μm NALGENE PTFE filters to remove any dust particles, prior to use.

Methods. Light scattering measurements were done using a Brookhaven goniometer equipped with a Coherent argon laser using the 514 nm line, an operating power of 20−100 mW, and a q range of 0.006−0.03 nm^{-1}. Using filtered solvent, all diblock solutions were prepared by weighing. After being placed under argon, to prevent oxidation, the samples were dissolved in heptane at 25 °C. The measurements were preformed with a concentration range from 10^{-7} to10^{-3} g/mL. Molecular weights and second virial coefficients were determined using the classic Zimm plot method.[18] Static light scattering (SLS) was employed to monitor the transformation between cylindrical to spherical micelles upon heating and the reverse transition upon cooling. For these measurements a full angle scan would take too long, as such the intensity of scattered light was measured at a fixed angle as a function of time and then converted to aggregation number using the angular dependence obtained from full angle scans. This is done by measuring the ratio of the intensity at a fixed angle to the intensity obtained by extrapolating to zero q for the sample before the morphological transition. It is then assumed that the ratio changes linearly throughout the morphological transition. By multiplying the scattering intensity measured at the fixed angle by the calculated ratio at that stage of the transition, a quasi-zero q extrapolated value can be obtained. Since the transition upon cooling is much slower, the classic Zimm plot method can be used to calculate the average aggregation number upon cooling. Sample morphology was confirmed through visualization of individual micelles by atomic force microscopy (AFM) using a Multimode microscope (Nanoscope IIIa, Veeco Metrology Group) and NCL Si probes (NANOSENSORS Switzerland). Samples for the AFM studies were prepared by spin-casting dilute polymer solutions at the desired temperature onto freshly cleaved mica.

Results and Discussion

In the performed experiments, the temperature was varied from 25 to 40 °C. This variation in temperature changes the solvent quality of heptane for both the PS and PI blocks. The change in the solvent quality for PI was measured through the variation in the second virial coefficient (A_2). We carried out A_2 measurements for a PI standard with a molecular weight of

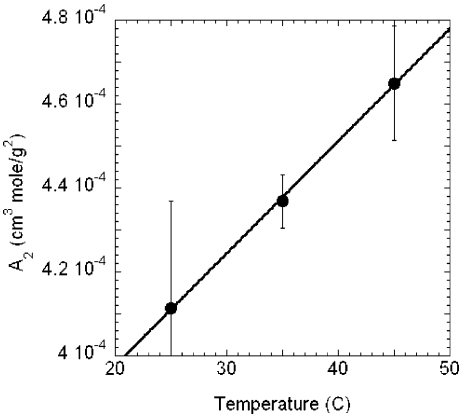

Figure 2. Temperature variation of the second virial coefficient of linear polyisoprene (34 kDa) in heptane. Fitting the data results in $A_2 = 3.4 \times 10^{-4} + 2.68 \times 10^{-6}(T - 273)$, where temperature T is in kelvin.

34 kDa at three different temperatures. As seen in Figure 2, the second virial coefficient of PI in heptane increases with temperature. By fitting these data and using the relationship $\nu = 2A_2M_0^2/(a_A{}^3N_{AV})$, where N_{AV} is Avogadro's number and M_0 is the molecular weight of the monomer,[18] one can calculate the variation in the excluded volume parameter with temperature as

$$\nu = 2M_0{}^2(3.4 \times 10^{-4} + 2.68 \times 10^{-6}(T - 273)) \times (\mathrm{cm}^3\,\mathrm{mol/g}^2)/(a_A{}^3N_{AV}) \quad (3)$$

In addition to the change in the excluded volume of the PI corona, it has been previously shown that the surface free energy γ for polystyrene in heptane varies with temperature[19] as

$$\gamma/kT = (0.68 \pm 0.01) - (5.2 \pm 0.2) \times 10^{-3}(T - 273) \quad (4)$$

where T is temperature in kelvin. By using the variation in ν and γ with temperature in eqs 1 and 2, the change in the morphological boundaries with temperature can be calculated. From eqs 3 and 4 one can also calculate the relative contribution of the change in solvent quality for the corona and core blocks in the boundary shift. If temperature increases 10 deg, the excluded volume parameter of the PI corona increases by $\Delta\nu/\nu = 0.025$, i.e., by 2.5%, while the surface energy of the PS core decreases as $\Delta\gamma/\gamma = -0.095$, i.e., by 9.5%. Since both parameters enter eqs 1 and 2 with the same power 1/3, this causes approximately $1/3(0.025 + 0.095) \times 100\% \cong 4\%$ shift of the boundaries to lower values of N_A, wherein the surface energy of the core has a dominant contribution ~4 times larger than that of corona. It is remarkable that this shift is significantly lower than the 18% relative standard deviation (RSD) of the blocks length due to the polydispersity calculated as $\mathrm{RSD} = \sqrt{\mathrm{PDI}-1} \cong \sqrt{1.035-1} = 0.18$. This strongly suggests that individual micelles include a mixture of diblocks with different molecular weights.

Figure 1 shows that as the temperature is raised from 25 to 35 or 40 °C, the morphological boundaries shift to lower values of N_A as shown by the dashed lines. This means that if a cylindrical micelle sample is just below the spherical−cylindrical (S−C) boundary at 25 °C, it will adopt a spherical morphology when the temperature is increased to 35 °C, and the phase boundary shifts below the point corresponding to the sample composition. Likewise, a vesicle sample near the cylindrical−vesicle (C−V) boundary at 25 °C will adopt a cylindrical morphology upon heating 40 °C when the phase boundary shifts below the composition of the actual sample.

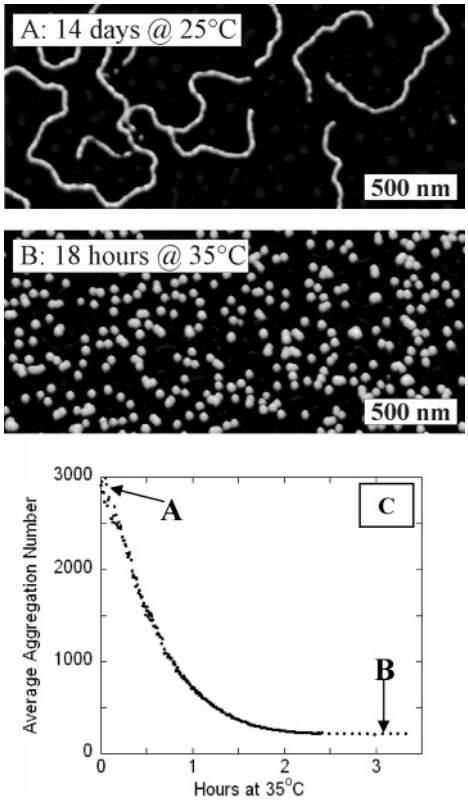

Figure 3. AFM height micrographs of PS-*b*-PI micelles with a PS block of 20.6 kDa, a PI block of 6 kDa, and a concentration of 0.42 mg/mL (sample 1). Micrograph A was taken after a solution of sample 1 had been equilibrated 25 °C for 2 weeks. Micrograph B was obtained from a solution that had been at 35 °C for 18 h. Plots C shows decay of the average aggregation number with time at 35 °C monitored by static light scattering. The scattering intensity was measured at a fixed angle and then converted to aggregation number.

These predictions were confirmed using two diblocks samples (Table 1) that were purposely synthesized to be in the proximity of the calculated S−C and C−V boundaries. Sample 1 with a PS block of 21.6 kDa and a PI block of 6 kDa was found to be near the S−C boundary (solid circle) and formed cylindrical micelles at 25 °C (Figure 3A). Since sample 1 is just below the boundary, only a small decrease in γ and/or an increase in ν is needed to cause the sample to become spherical. When the sample is heated to 35 °C, only spherical micelles are observed (Figure 3B). To make sure that the adsorption procedure and interactions with the surface are not influencing the observed morphologies, light scattering was used to monitor and confirm the morphological transition. Figure 3C shows the decay in the average aggregation number (the number of diblocks associating to form the micelle) after the solution has been heated to 35 °C. As seen in the figure, the average aggregation number drops from ~3000 to 200 in a little over 2 h. This change in the average aggregation number is consistent with the AFM images, which show a change from long cylindrical micelles (Figure 3A) to small spherical ones (Figure 3B).

Upon subsequent cooling back to 25 °C cylindrical micelles were once again observed (Figure 4A−C). However, the growth of cylindrical micelles appears to take a much longer time than the decay of cylindrical micelles into spherical ones. As seen in Figure 4A, after keeping the solution for 4 days at 25 °C only a few short cylindrical micelles were observed, and most of the micelles still had a spherical morphology. Equilibrating

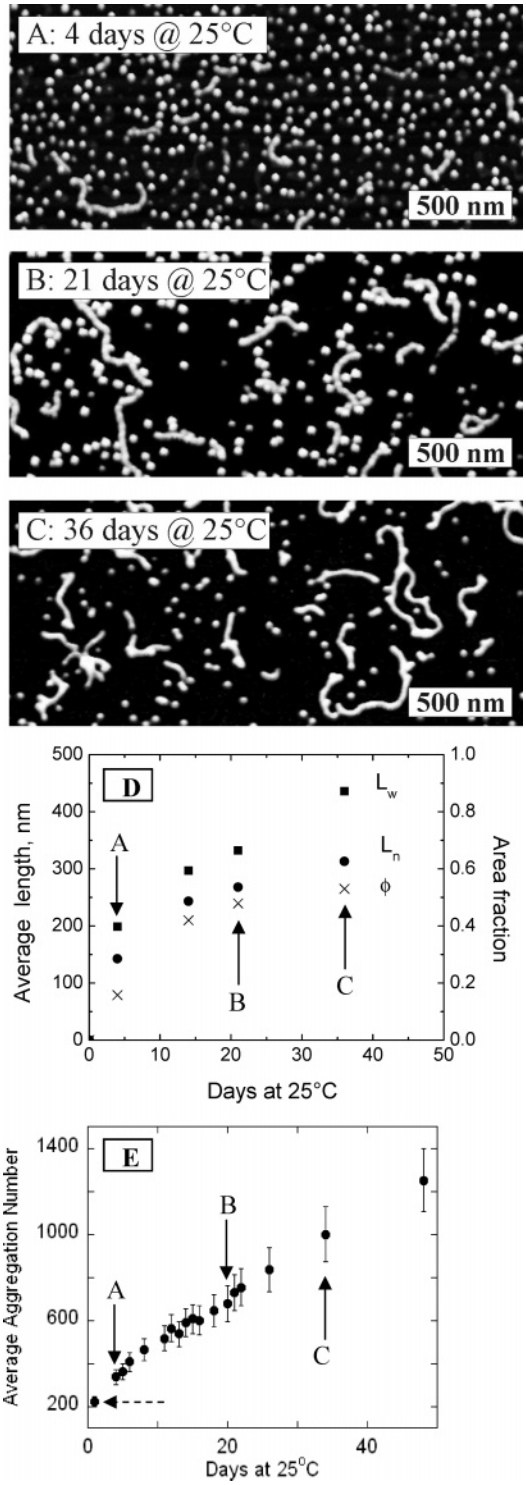

Figure 4. AFM height images A, B, and C were obtained from sample 1 that was spin-cast after the solution had been cooled back from 35 to 25 °C and then kept at 25 °C for 4, 21, and 36 days, respectively. Plot D demonstrates the increase of the fraction of the surface coverage of cylindrical micelles (crosses) along with their number-average contour length (circles) and length average contour length (squares) for sample 1 after cooling from 35 to 25 °C. Complementary to the AFM data, plot E shows evolution of the average aggregation number with time at 25 °C measured by static light scattering. The aggregation numbers for plot E were measured using the classic Zimm plot method. The letter labels in plots D and E indicate the corresponding AFM images in A−C. The dashed arrow in E points to the original solution of spherical micelles equilibrated at 35 °C for 18 h (Figure 3B).

the solution at 25 °C for a longer period of time resulted in the length and fraction of cylindrical micelles to increase as seen

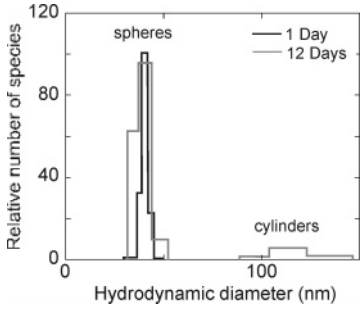

Figure 5. Size distribution was measured for sample 1 after being at 25 °C for 1 day (black line) and 12 days (gray line) using the Contin fit of dynamic light scattering data. The plot takes into account the higher scattering intensity from the cylindrical micelles and shows the relative number of cylindrical vs spherical species, not just the scattering intensity. In addition to spherical micelles having a hydrodynamic diameter of ∼40 nm, the bimodal distribution after 12 days indicates the presence of a second larger species. This is consistent with the AFM observation of coexistence of spherical and cylindrical micelles during the slow equilibration process at 25 °C.

in Figure 4B,C. It should be noted that the small difference in micelle morphology observed between the AFM images can be ascribed to variations in the shape and sharpness of the AFM tips that were used to capture the images. By using AFM, the fraction of the surface area covered by cylindrical micelles vs the total surface coverage of all micelle morphologies along with the number- and weight-average lengths (L_n and L_w) of cylindrical micelles were independently measured. As seen in Figure 4D, both the fraction of coverage (crosses) and the average length (circles and squares) are still increasing after several weeks at 25 °C, unlike the rapid relaxation from cylinders to spheres at a higher temperature of 35 °C (Figure 3C). While the sample has still not reached a completely cylindrical conformation after 36 days, it appears that the sample is slowly returning to a completely cylindrical conformation.

To verify the AFM measurements of micelles adsorbed onto surface, light scattering was used to follow the slow growth of cylindrical micelles in solution. As seen in Figure 4E, the average aggregation number is still increasing after the solution has been kept at 25 °C for several weeks. This observation is consistent with the gradual increase of the weight-average length of cylindrical micelles (squares in Figure 4D), when it is taken into account that light scattering is measuring the weight-average mass of all micelle species present in solution. In addition, dynamic light scattering was used to confirm the presence of different sized species in solution after cooling back to 25 °C. Figure 5 shows that upon cooling a bimodal size distribution emerges in the CONTIN fit of dynamic light scattering data.[20] This indicates that, in addition to the spheres characterized by a monomodal distribution at 35 °C, a second type of species with a larger hydrodynamic diameter forms upon cooling to 25 °C. On the basis of the AFM observations, the second species is ascribed to cylindrical micelles.

In a similar way, we studied a reversible transition from cylindrical micelles to vesicles. Sample 2 with the same PS block of 21.6 kDa and a shorter PI block of 4 kDa was found to be near the calculated cylindrical−vesicle boundary (Figure 1). At room temperature, it was found to be just below the boundary and therefore comprised of mostly vesicles. The AFM image in Figure 6A shows the expected morphology of vesicles that have collapsed onto a solid substrate to form a disklike structure with the characteristic wrinkles and wedgelike cuts. The cross-sectional profile in Figure 6B demonstrates that the thickness of the collapsed vesicles is approximately twice the thickness of the cylindrical micelles (Figure 6D), which is

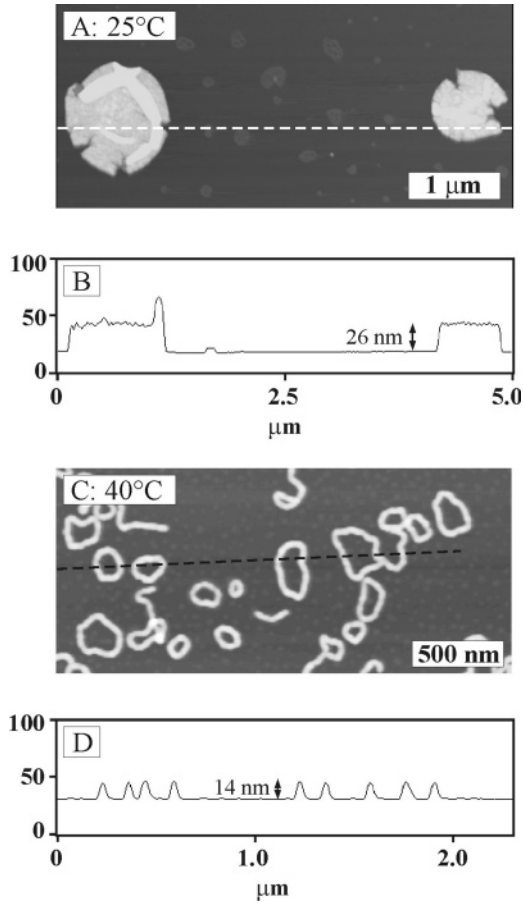

Figure 6. AFM height images of sample 2 prepared from a micellar solution with a concentration of 0.33 mg/mL equilibrated at different temperatures. Collapsed vesicles in A were observed after the sample had been kept at 25 °C for 2 weeks. Vesicles transformed into cylindrical micelles of both linear and mostly ringlike morphologies when temperature was raised to 40 °C (imaged C). Figure B is the cross-sectional analysis along the dashed line in image A. The vertical distance between the two arrows is 26 nm, which is approximately twice the height of the cylindrical micelles in C. Cylindrical rings in C were spin-cast from a 40 °C solution. The cross-sectional profile in D was measured along the dashed line in image C in order to demonstrate that cylindrical micelles have a thickness of 14 nm.

consistent with the bilayer structure expected for vesicles. For sample 2, it was necessary to heat the sample from 25 to 40 °C before vesicles were no longer seen (Figure 6C). It was also observed with sample 2 that the cylindrical micelles near the vesicle boundary appear to favor the formation of rings. This makes sense since the end-caps of cylinders have a spherical geometry. As the micelles get closer to the vesicle boundary, the energy cost of these spherical end-caps becomes higher. Thus, it is favorable for the cylindrical micelles to either form very long cylinders or rings in order to reduce the number of end-caps.[21,22]

Upon cooling back to 25 °C, vesicles are once again observed (Figure 7A). As with the growth of cylindrical micelles of sample 1, the vesicle solution appears to be slowly returning to the original all-vesicle conformation. However, vesicles are now found to coexist with small toroidal micelles having almost the same cross section as the cylindrical micelles observed at 40 °C (Figure 6C). Although small toroidal micelles are reproducibly observed in this work for PS-*b*-PI diblocks as well as for triblock copolymers,[23] their origin is not understood at this time. The observed diblock toroids could either be just a lower weight fraction of ringlike micelles seen in Figure 6C or correspond

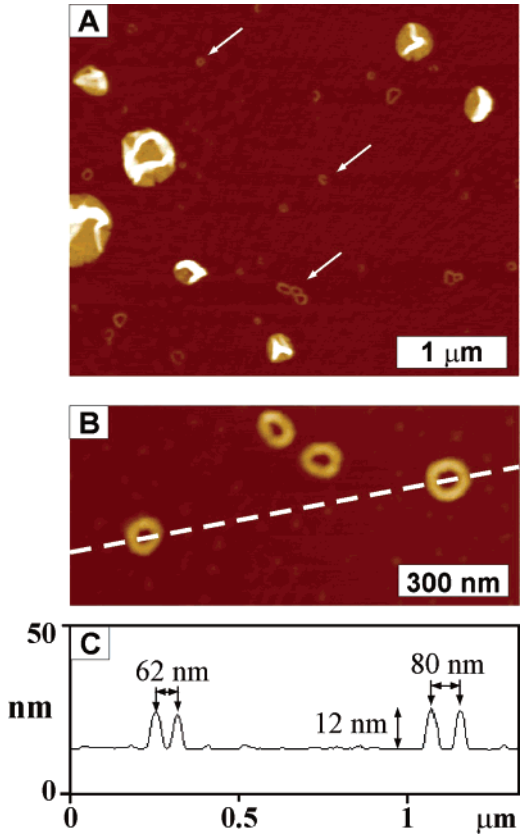

Figure 7. AFM height image A demonstrates the coexistence of small toroidal micelles (arrows) and vesicles when a solution of sample 2 (PS-*b*-PI diblock with a PS block of 20.6 kDa and a PI block of 4.3 kDa) in heptane was cooled from 40 °C (Figure 6C) back to 25 °C (sample 2). Image B gives higher magnification of toroidal micelles observed in A. The cross-sectional profile in C presents typical dimensions of the toroids.

to a new metastable state given to their distinctively high curvature and a relatively uniform diameter of ca. 70 nm.

Conclusions

We have demonstrated reversible morphological phase transitions induced solely by temperature for polystyrene-*b*-polyisoprene micelles in heptane. Upon heating from 25 to 40 °C cylindrical micelles are changed to spherical micelles and vesicle micelles are converted to cylindrical micelles. Upon cooling back to 25 °C, the original morphologies are once again observed; however, the growth rates of the cylindrical and vesicle micelles are seen to be much slower than the rate of dissolution at higher temperatures—possibly a result of slow kinetics near the glass transition temperature T_g. Through the observation of the two transitions, we confirmed the universal width of the cylindrical range which was predicted.[6] An in-depth examination of the kinetics and measurements of the T_g will be the subject of future work.

Acknowledgment. We thank the National Science Foundation NIRT ECS-0103307 for funding and the STC Program of the National Science Foundation under Agreement CHE-9876674 for funding and shared facilities. M.P. and N.H. are grateful to the Research Committee of the University of Athens for financial support.

References and Notes

(1) Tuzar, Z.; Kratochvil, P. *Adv. Colloid Interface Sci.* **1976**, *6*, 201.

(2) Hamley, I. W. *The Physics of Block Copolymers*; Oxford Universtity Press: Oxford, England, 1998.
(3) Tuzar, Z.; Kratochvil, P. *Surf. Colloid Sci.* **1993**, *15*, 1.
(4) Halperin, A.; Tirrell, M.; Lodge, T. P. *Adv. Polym. Sci.* **1992**, *100*, 31.
(5) Chocair, A.; Eisenberg, A. *Eur. Phys. J. E* **2003**, *10*, 37.
(6) Zhulina, E. B.; Adam, M.; LaRue, I.; Sheiko, S. S.; Rubinstein, M. *Macromolecules* **2005**, *38*, 5330.
(7) Price, C. *Pure Appl. Chem.* **1983**, *55*, 1563.
(8) Won, Y. Y.; Brannan, A. K.; Davis, H. T.; Bates, F. S. *J. Phys. Chem. B* **2002**, *106*, 3354.
(9) Jain, S.; Bates, F. S. *Science* **2003**, *300*, 460.
(10) Nakano, M.; Matsuoka, H.; Yamaoka, H.; Poppe, A.; Richter, D. *Macromolecules* **1999**, *32*, 697.
(11) LaRue, I.; Adam, M.; da Silva, M.; Sheiko, S. S.; Rubinstein, M. *Macromolecules* **2004**, *37*, 5002.
(12) Ouarti, N.; Viville, P.; Lazzaroni, R.; Minatti, E.; Schappacher, M.; Deffieux, A.; Borsali, R. *Langmuir* **2005**, *21*, 1180.
(13) Zhang, L; Eisenberg, A. *Macromolecules* **1999**, *32*, 2239.
(14) Lodge, T. P.; Bang, J.; Li, Z.; Hillmyer, M. A.; Talmon, Y. *R. Soc. Chem., Faraday Discuss.* **2005**, *128*, 1.
(15) Ding, J.; Liu, G.; Yang, M. *Polymer* **1997**, *38*, 5497.
(16) Hu, Z.; Jonas, A. M.; Varshney, S. K.; Gohy, J. F. *J. Am. Chem. Soc.* **2005**, *127*, 6526.
(17) Hadjichristidis, N.; Iatrou, H.; Pispas, S.; Pitsikalis, M. *J. Polym. Sci., Part A: Polym. Chem.* **2000**, *38*, 3211.
(18) Rubinstein, M.; Colby, R. H. *Polymer Physics*; Oxford University Press: Oxford, UK, 2003.
(19) Lairez, D.; Adam, M.; Carton, J.-P.; Raspaud, E. *Macromolecules* **1997**, *30*, 6798.
(20) Provencher, S. W. *Makromol. Chem.* **1979**, *180*, 201.
(21) Israelachvili, J. *Intermolecular & Surface Forces*; Academic Press: San Diego, 2000.
(22) May, S.; Ben-Shaul, A. *J. Phys. Chem. B* **2001**, *105*, 630.
(23) Pochan, D. J.; Chen, Z.; Cui, H.; Hales, K.; Qi, K.; Wooley, K. L. *Science* **2004**, *306*, 94.

MA051548Z